Journal of Organometallic Chemistry, 342 (1988) 215–233
Elsevier Sequoia S.A., Lausanne – Printed in The Netherlands

Nature of the hydrogen bridge in transition metal complexes

II *. Molecular orbital calculations of binuclear carbonyls of Mn, Re, Cr, Mo and W with double hydrogen bridges

Bogusława Jeżowska-Trzebiatowska and Barbara Nissen-Sobocińska

Institute for Low Temperature and Structure Research, Polish Academy of Sciences, Plac Katedralny 1, 50-950 Wrocław (Poland)

(Received September 15th, 1987)

Abstract

To throw more light on the nature and character of the metal–hydrogen–metal bond we carried out the electronic structure calculations by use of the parameter-free Fenske-Hall method and the semi-empirical EHT method for 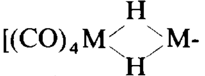 $[(CO)_4M\overset{H}{\underset{H}{\langle\;\rangle}}M(CO)_4]^n$ complexes (M = Mn, Re, Cr, Mo, W and $n = -2,0$). The character and stability of the double hydrogen bridges in these complexes and in 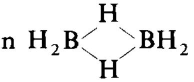 $H_2B\overset{H}{\underset{H}{\langle\;\rangle}}BH_2$ and 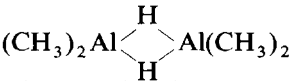 $(CH_3)_2Al\overset{H}{\underset{H}{\langle\;\rangle}}Al(CH_3)_2$ were compared. The effects that type of transition metal has on the character and stability of double hydrogen bridges in carbonyl dimers are described. The electronic structures of the bridge cores in the double- and single-hydrogen bridge binuclear carbonyls of chromium and molybdenum were compared.

Introduction

Up to now the group of known transition metal complexes containing the metal–hydrogen–metal bridge bond is quite large and includes various types of hydrogen-bridged metal systems. In our previous paper [1] we described the character and stability of single-hydrogen-bridged binuclear carbonyls which were evident from the results of molecular orbital calculations carried out by use of the parameter-free Fenske-Hall method [2].

---

* For part I see Ref. 1.

Our studies were on double-hydrogen-bridged binuclear transition metal carbonyls. It is noteworthy that all the metals of the VIB group: Cr, Mo and W form stable carbonyl dimers with single hydrogen bridges of the $[(CO)_5M{-}H{-}M(CO)_5]^-$ type [3] which were thoroughly examined by the X-ray and neutron diffraction methods. However, the complex with the double hydrogen bridge, of the type $[(CO)_4M\overset{H}{\underset{H}{<\;>}}M(CO)_4]^{2-}$ was studied by X-ray crystallography only for tungsten [4]. A similar system is found in the rhenium compound, viz. $(CO)_4Re\overset{H}{\underset{H}{<\;>}}Re(CO)_4$ [5].

Mixed double bridges, in which hydrogen and phosphine participate in the bridge bonds, have been found in molybdenum $(CO)_2(C_5H_5)$-$Mo\overset{P(Me)_2}{\underset{H}{<\;>}}Mo(C_5H_5)(CO)_2$ [6], and manganese $(CO)_4Mn\overset{PPh_2}{\underset{H}{<\;>}}Mn(CO)_4$ [7] complexes.

Up to now however, no carbonyl complex containing bridge cores of the types $M\overset{H}{\underset{H}{<\;>}}M$ or $M\overset{H}{\underset{L}{<\;>}}M$ has been found for chromium.

In this paper we show to what extent the character and stability of double hydrogen bridges in the $[(CO)_4M\overset{H}{\underset{H}{<\;>}}M(CO)_4]^n$ complexes depends on the type of metal. We will also compare the electronic structure of double hydrogen bridges in the $[(CO)_4M\overset{H}{\underset{H}{<\;>}}M(CO)_4]^{2-}$ complexes with that of single hydrogen bridges in $[(CO)_5M{-}H{-}M(CO)_5]^-$ complexes, where M = Cr, Mo, which have been described in detail previously [1].

Thus we have carried out electronic structure calculations for the following isoelectronic carbonyl complexes with double hydrogen bridges:

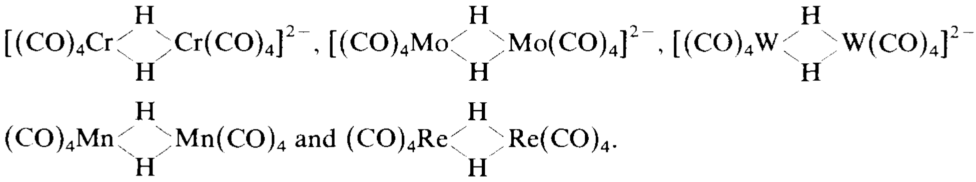

$$[(CO)_4Cr\overset{H}{\underset{H}{<\;>}}Cr(CO)_4]^{2-},\ [(CO)_4Mo\overset{H}{\underset{H}{<\;>}}Mo(CO)_4]^{2-},\ [(CO)_4W\overset{H}{\underset{H}{<\;>}}W(CO)_4]^{2-},$$

$$(CO)_4Mn\overset{H}{\underset{H}{<\;>}}Mn(CO)_4 \text{ and } (CO)_4Re\overset{H}{\underset{H}{<\;>}}Re(CO)_4.$$

For all these systems we have assumed a somewhat idealized D_{2h} symmetry. It should be mentioned that Hoffman et al. have already found that for complexes with double hydrogen bridges the eclipsed conformation with D_{2h} symmetry is more stable than the staggered conformation with D_{2d} symmetry [8].

To the complexes of chromium, molybdenum and manganese we have applied the parameter-free Fenske-Hall method with the use of suitably optimized $1s,2s$ functions of the C and O atoms, $1s,2s,2p,\ldots,(n-1)d,ns,np$ functions of the metal atoms and $1s$ of the hydrogen atom.

Calculations for the complexes of tungsten and rhenium were carried out by the extended Hückel method (EHT). This method was regarded as complementary because of the lack of atomic functions for calculations for the third row transition elements by the Fenske-Hall method.

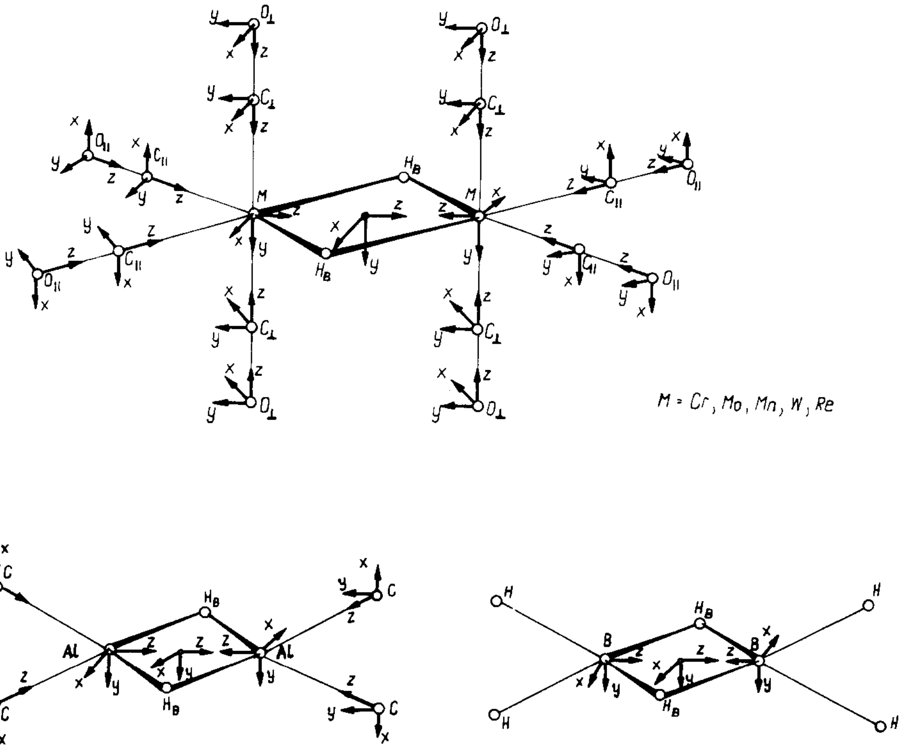

Fig. 1. (a) Coordinate systems assumed in calculations for the $[(CO)_4M\overset{H}{\underset{H}{<\!>}}M(CO)_4]^n$ complexes. (b) Coordinate systems assumed in calculations for the $(CH_3)_2Al\overset{H}{\underset{H}{<\!>}}Al(CH_3)_2$ and $H_2B\overset{H}{\underset{H}{<\!>}}BH_2$.

In order to provide a reference point for comparison of the electronic structure of all the complexes under investigation, the EHT method was also applied to the molybdenum complex. Figure 1a shows the local coordinate systems about the atoms assumed for calculations by the Fenske-Hall and the EHT methods respectively and Table 1 lists the bond lengths.

The structural parameters for tungsten and rhenium complexes correspond to the values determined experimentally [4,5] but for molybdenum and manganese complexes the parameters were such that they were in accord with the X-ray diffraction data for known complexes with mixed bridges [6,7].

For the calculations the chromium complex was assumed to have structural parameters similar to those of molybdenum complex. The metal–hydrogen–metal bonds which occur in transition metal complexes may be compared with B–H–B and Al–H–Al bonds. Calculations by use of the Fenske-Hall method were also carried out for diborane $H_2B\overset{H}{\underset{H}{<\!>}}BH_2$ [9] and dimethyl hydride aluminium dimer $(CH_3)_2Al\overset{H}{\underset{H}{<\!>}}Al(CH_3)_2$ [10].

Table 1
Structural parameters used in the calculations

Compound	Bond lengths (Å)			Ref.
	M–M	M–H	M–CO	
$(CO)_4Mn\overset{H}{\underset{H}{\langle\;\rangle}}Mn(CO)_4$	2.937	1.86	1.79	6
$[(CO)_4Cr\overset{H}{\underset{H}{\langle\;\rangle}}Cr(CO)_4]^{2-}$	3.267	1.86	1.96	7
$[(CO)_4Mo\overset{H}{\underset{H}{\langle\;\rangle}}Mo(CO)_4]^{2-}$	3.267	1.86	1.96	7
$[(CO)_4W\overset{H}{\underset{H}{\langle\;\rangle}}W(CO)_4]^{2-}$	3.062	1.86	1.90	4
$(CO)_4Re\overset{H}{\underset{H}{\langle\;\rangle}}Re(CO)_4$	2.896	1.86	1.99	5
	Al–Al	Al–H	Al–CH$_3$	
$(CH_3)_2Al\overset{H}{\underset{H}{\langle\;\rangle}}Al(CH_3)_2$	2.617	1.676	1.947	10
	B–B	B–H$_B$ [a]	B–H$_T$ [b]	
$H_2B\overset{H}{\underset{H}{\langle\;\rangle}}BH_2$	1.772	1.339	1.191	9

[a] H$_B$ = bridge hydrogen atom. [b] H$_T$ = terminal hydrogen atom.

Figure 1b shows the coordinate systems of atoms. Table 1 lists the structural parameters, which were assumed for the calculations, were consistent with X-ray diffraction data for these compounds.

Results and discussion

Electronic structure of the $[(CO)_4M\overset{H}{\underset{H}{\langle\;\rangle}}M(CO)_4]^n$ complexes determined by use of the Fenske-Hall method

The filled energy levels which result from the valence atomic orbitals of O,C,M and H for the $[(CO)_4Cr\overset{H}{\underset{H}{\langle\;\rangle}}Cr(CO)_4]^{2-}$, $[(CO)_4Mo\overset{H}{\underset{H}{\langle\;\rangle}}Mo(CO)_4]^{2-}$ and $(CO)_4Mn\overset{H}{\underset{H}{\langle\;\rangle}}Mn(CO)_4$ complexes examined by use of the Fenske-Hall method can be grouped as follows:

(1) the lowest levels of exclusively σ-type molecular orbitals of the CO groups,
(2) intermixed levels of varying character:
  (a) levels of exclusively σ-type MOs of the CO groups,
  (b) levels of exclusively π^b-type MOs of the CO groups,

Table 2

Energies and compositions of highest occupied molecular energy levels of 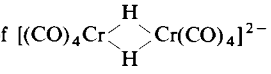 $[(CO)_4Cr\underset{H}{\overset{H}{<\!>}}Cr(CO)_4]^{2-}$ with D_{2h} symmetry calculated by use of the Fenske-Hall method

MO	Energy (eV)	Greatest contributions by the valence atomic orbitals (%)					
$6b_{2g}$ LUMO	−9.54	$p_x(C_\parallel)$	45	$p_x(O_\perp)$	25	$3d_{xz}(Cr)$	13
$10a_g$ HOMO	−12.31	$p_y(O_\parallel)$	39	$3d_{z^2}(Cr)$	12	$3d_{x^2-y^2}(Cr)$	12
$9b_{1u}$	−12.52	$p_y(O_\parallel)$	43	$3d_{z^2}(Cr)$	26	$3d_{x^2-y^2}(Cr)$	14
$6b_{3g}$	−12.62	$3d_{yz}(Cr)$	40	$p_y(O_\perp)$	27	$p_x(O_\parallel)$	13
$6b_{3u}$	−12.87	$s(H_B)$	57	$3d_{z^2}(Cr)$	7	$p_z(C_\parallel)$	6
$6b_{2u}$	−12.98	$3d_{yz}(Cr)$	37	$p_y(O_\perp)$	33	$p_x(O_\parallel)$	13
$3a_u$	−13.00	$3d_{xy}(Cr)$	38	$p_x(O_\perp)$	30	$p_x(O_\parallel)$	19
$3b_{1g}$	−13.03	$3d_{xy}(Cr)$	38	$p_x(O_\perp)$	29	$p_x(O_\parallel)$	19
$9a_g$	−14.67	$s(H_B)$	60	$3d_{z^2}(Cr)$	17	$p_y(O_\perp)$	7
$5b_{2u}$	−15.76	$p_x(O_\parallel)$	45	$p_z(C_\perp)$	20	$p_z(O_\perp)$	13
$5b_{3g}$	−15.78	$p_x(O_\parallel)$	45	$p_z(C_\perp)$	19	$p_z(O_\perp)$	14
$2a_u$	−16.48	$p_x(O_\parallel)$	46	$p_x(O_\perp)$	29	$p_x(C_\parallel)$	17
$5b_{2g}$	−16.48	$p_y(O_\parallel)$	69	$p_y(C_\parallel)$	26	$3d_{xz}(Cr)$	2
$2b_{1g}$	−16.49	$p_y(O_\parallel)$	47	$p_x(O_\perp)$	28	$p_x(C_\parallel)$	18
$5b_{3u}$	−16.52	$p_y(O_\parallel)$	68	$p_y(C_\parallel)$	27	$s(O_\perp)$	2
$8b_{1u}$	−16.72	$p_y(O_\perp)$	67	$p_y(C_\perp)$	25	$p_z(C_\parallel)$	2

(c) levels corresponding to the bonding interactions of σ-type MOs from the CO groups with the d orbitals of the metal atoms, i.e. σ–dM interactions,

(d) levels corresponding to the bonding interactions of π^b-type MOs of the CO groups with the d orbitals of the metal atoms, i.e. π^b–dM interactions,

(3) two levels ($9a_g$, $6b_{3u}$), mainly AOs of the bridging hydrogen atoms and metal atoms, which correspond to the M–H–M bridge bonds,

(4) the highest filled levels of the π^a-type MOs of the CO groups and d-type orbitals of the metal atoms, which correspond to the $\pi^a \rightarrow d$M bonding interactions.

Tables 2, 3 and 4 list the energy values and percentage compositions of the energy levels of groups 3 and 4.

A correlation of these energy levels for three of the discussed complexes is depicted in Fig. 2. The electronic structures of these complexes have one property in common, viz., the same degree of delocalization of the 1s AOs of the bridging hydrogen atoms participating in the formation of only two, filled, bonding molecular levels: $9a_g$ and $6b_{3u}$ (Tables 2, 3, 4).

The bridge molecular levels are delocalized over the entire molecule since the atomic orbitals of H,M,C and O are involved in their formation. The highest contribution to the bridge molecular levels $9a_g$ and $6b_{3u}$ is provided by the atomic orbitals of hydrogen, it is equal more than 50% for all three complexes in question.

The contribution by the atomic orbitals of metal in the $9a_g$ and $6b_{3u}$ levels is relatively low for molybdenum and chromium complexes and slightly higher for the manganese complex.

As a measure of the stability of a double hydrogen bridge in the 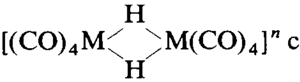 $[(CO)_4M\underset{H}{\overset{H}{<\!>}}M(CO)_4]^n$ complexes we assumed that there is an energy difference

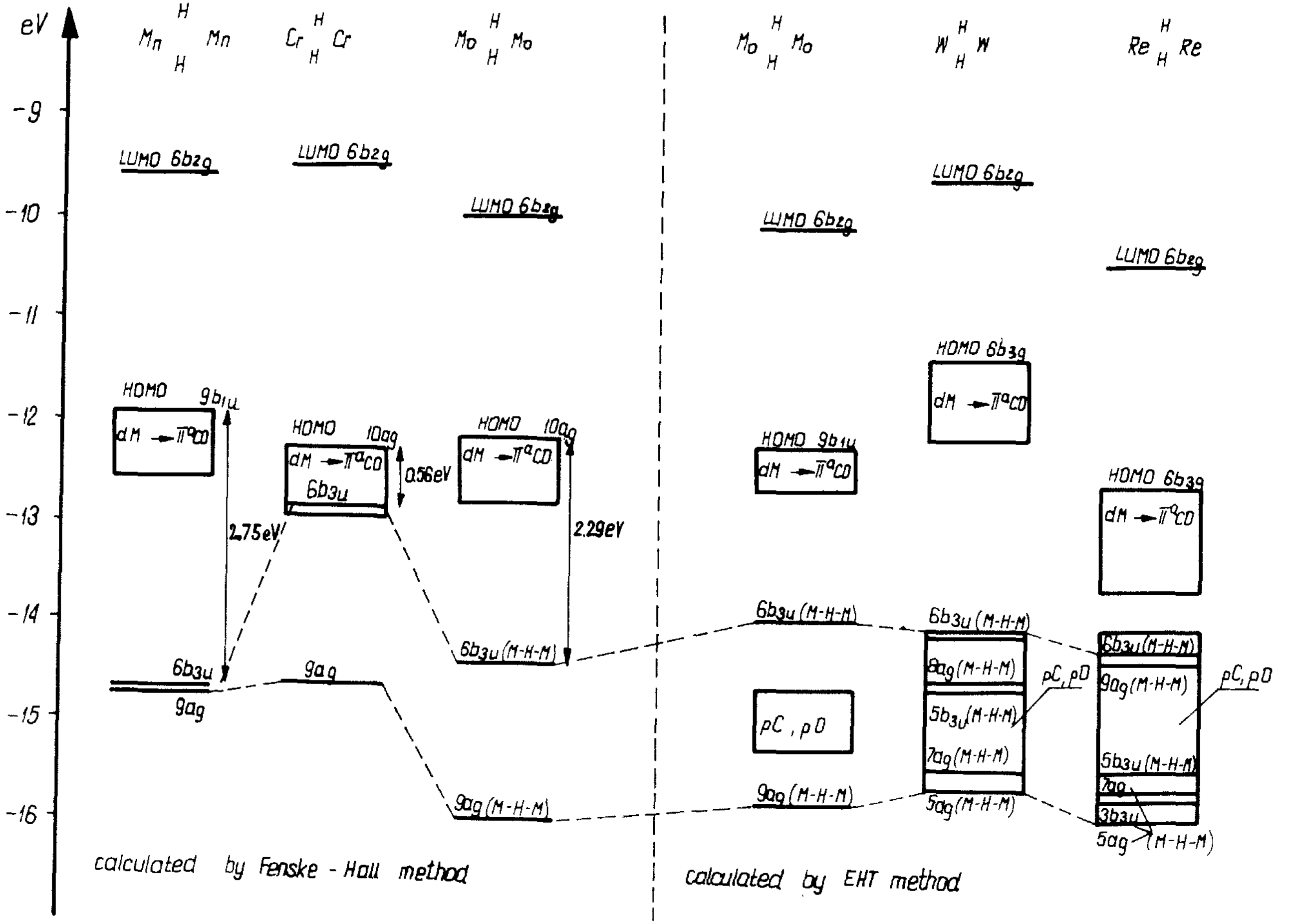

Fig. 2. Correlation of the molecular energy levels of the carbonyl dimers of Mn, Cr, Mo, W and Re with double hydrogen bridges.

Table 3

Energies and compositions of highest occupied molecular energy levels of $[(\mathrm{CO})_4\mathrm{Mo}\overset{\mathrm{H}}{\underset{\mathrm{H}}{\langle\rangle}}\mathrm{Mo(CO)}_4]^{2-}$ with D_{2h} symmetry calculated by use of the Fenske-Hall method

MO	Energy (eV)	Greatest contributions by the valence atomic orbitals (%)					
$6b_{2g}$ LUMO	−9.96	$p_x(\mathrm{O}_\perp)$	45	$p_x(\mathrm{C}_\perp)$	35	$4d_{xz}(\mathrm{Mo})$	20
$10a_g$ HOMO	−12.19	$p_y(\mathrm{O}_\parallel)$	50	$4d_{z^2}(\mathrm{Mo})$	18	$p_y(\mathrm{C}_\parallel)$	17
$9b_{1u}$	−12.23	$p_y(\mathrm{O}_\parallel)$	45	$4d_{z^2}(\mathrm{Mo})$	20	$p_y(\mathrm{C}_\parallel)$	17
$6b_{3g}$	−12.47	$4d_{yz}(\mathrm{Mo})$	35	$p_y(\mathrm{O}_\perp)$	29	$p_x(\mathrm{O}_\parallel)$	17
$3a_u$	−12.73	$4d_{xy}(\mathrm{Mo})$	33	$p_x(\mathrm{O}_\perp)$	30	$p_x(\mathrm{O}_\parallel)$	21
$6b_{2u}$	−12.74	$p_y(\mathrm{O}_\perp)$	34	$4d_{yz}(\mathrm{Mo})$	32	$p_x(\mathrm{O}_\parallel)$	16
$3b_{1g}$	−12.75	$4d_{xy}(\mathrm{Mo})$	32	$p_x(\mathrm{O}_\perp)$	31	$p_x(\mathrm{O}_\parallel)$	21
$6b_{3u}$	−14.48	$s(\mathrm{H_B})$	54	$p_x(\mathrm{Mo})$	16	$p_x(\mathrm{O}_\perp)$	8
$9a_g$	−16.07	$s(\mathrm{H_B})$	54	$p_y(\mathrm{O}_\perp)$	15	$p_z(\mathrm{Mo})$	12
$5b_{3g}$	−16.09	$p_x(\mathrm{O}_\parallel)$	55	$p_x(\mathrm{C}_\parallel)$	17	$p_y(\mathrm{O}_\perp)$	17
$5b_{2u}$	−16.10	$p_x(\mathrm{O}_\parallel)$	56	$p_x(\mathrm{C}_\parallel)$	17	$p_y(\mathrm{O}_\perp)$	13
$5b_{2g}$	−16.24	$p_y(\mathrm{O}_\parallel)$	70	$p_y(\mathrm{C}_\parallel)$	27	$4d_{xz}(\mathrm{Mo})$	1
$5b_{3u}$	−16.29	$p_y(\mathrm{O}_\parallel)$	68	$p_y(\mathrm{C}_\parallel)$	28	$p_x(\mathrm{O}_\perp)$	1
$2a_u$	−16.32	$p_x(\mathrm{O}_\parallel)$	49	$p_x(\mathrm{O}_\perp)$	26	$p_x(\mathrm{C}_\parallel)$	21
$2b_{1g}$	−16.33	$p_x(\mathrm{O}_\parallel)$	49	$p_x(\mathrm{O}_\perp)$	25	$p_x(\mathrm{C}_\parallel)$	21
$8b_{1u}$	−16.75	$p_y(\mathrm{O}_\perp)$	67	$p_y(\mathrm{C}_\perp)$	26	$p_y(\mathrm{O}_\parallel)$	1

between the highest filled molecular level (HOMO) and the bridge molecular level $6b_{3u}$.

Stabilization energies of the $6b_{3u}$ orbital with regard to the HOMO orbital are

Table 4

Energies and compositions of highest occupied molecular levels of $(\mathrm{CO})_4\mathrm{Mn}\overset{\mathrm{H}}{\underset{\mathrm{H}}{\langle\rangle}}\mathrm{Mn(CO)}_4$ with D_{2h} symmetry calculated by use of the Fenske-Hall method

MO	Energy (eV)	Greatest contributions by the valence atomic orbitals (%)					
$6b_{2g}$ LUMO	−9.60	$3d_{xz}(\mathrm{Mn})$	45	$p_x(\mathrm{Mn})$	18	$p_y(\mathrm{O}_\parallel)$	15
$9b_{1u}$ HOMO	−11.94	$p_y(\mathrm{O}_\perp)$	40	$3d_{z^2}(\mathrm{Mn})$	33	$3d_{x^2-y^2}(\mathrm{Mn})$	15
$6b_{3g}$	−11.98	$3d_{yz}(\mathrm{Mn})$	64	$p_x(\mathrm{O}_\parallel)$	17	$p_y(\mathrm{O}_\perp)$	12
$10a_g$	−12.10	$p_y(\mathrm{C}_\parallel)$	40	$3d_{z^2}(\mathrm{Mn})$	34	$3d_{x^2-y^2}(\mathrm{Mn})$	13
$3a_u$	−12.39	$3d_{xy}(\mathrm{Mn})$	56	$p_x(\mathrm{O}_\parallel)$	24	$p_x(\mathrm{O}_\perp)$	12
$3b_{1g}$	−12.45	$3d_{xy}(\mathrm{Mn})$	55	$p_x(\mathrm{O}_\parallel)$	24	$p_x(\mathrm{O}_\perp)$	12
$6b_{2u}$	−12.58	$3d_{yz}(\mathrm{Mn})$	57	$p_x(\mathrm{O}_\parallel)$	20	$p_y(\mathrm{O}_\perp)$	14
$6b_{3u}$	−14.69	$s(\mathrm{H_B})$	51	$p_x(\mathrm{Mn})$	15	$3d_{xz}(\mathrm{Mn})$	13
$9a_g$	−14.74	$s(\mathrm{H_B})$	58	$p_z(\mathrm{Mn})$	19	$3d_{z^2}(\mathrm{Mn})$	13
$5b_{3g}$	−16.48	$p_x(\mathrm{O}_\parallel)$	59	$p_x(\mathrm{C}_\parallel)$	22	$3d_{yz}(\mathrm{Mn})$	3
$5b_{2u}$	−16.54	$p_x(\mathrm{O}_\parallel)$	55	$p_x(\mathrm{C}_\parallel)$	22	$3d_{yz}(\mathrm{Mn})$	6
$5b_{2g}$	−16.62	$p_y(\mathrm{O}_\parallel)$	66	$p_y(\mathrm{C}_\parallel)$	30	$3d_{xz}(\mathrm{Mn})$	1
$5b_{3u}$	−16.70	$p_y(\mathrm{O}_\parallel)$	58	$p_y(\mathrm{C}_\parallel)$	32	$p_z(\mathrm{O}_\parallel)$	3
$2a_u$	−17.07	$p_x(\mathrm{O}_\parallel)$	53	$p_x(\mathrm{C}_\parallel)$	35	$3d_{xy}(\mathrm{Mn})$	5
$2b_{1g}$	−17.08	$p_x(\mathrm{O}_\parallel)$	53	$p_x(\mathrm{C}_\parallel)$	36	$3d_{xy}(\mathrm{Mn})$	6
$8b_{1u}$	−17.52	$p_y(\mathrm{C}_\parallel)$	30	$p_z(\mathrm{O}_\parallel)$	24	$p_y(\mathrm{O}_\parallel)$	22

Table 5
Stability of the double hydrogen bridge

	$\Delta E_{\mathrm{HOMO},6b_{3u}}$ (eV)
Calculated by use of the Fenske-Hall method	
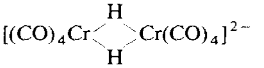 $[(CO)_4Cr\overset{H}{\underset{H}{<\,>}}Cr(CO)_4]^{2-}$	0.56
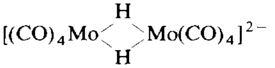 $[(CO)_4Mo\overset{H}{\underset{H}{<\,>}}Mo(CO)_4]^{2-}$	2.29
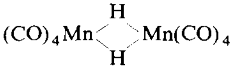 $(CO)_4Mn\overset{H}{\underset{H}{<\,>}}Mn(CO)_4$	2.75
Calculated by use of the EHT method	
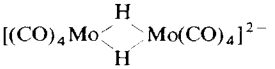 $[(CO)_4Mo\overset{H}{\underset{H}{<\,>}}Mo(CO)_4]^{2-}$	1.66
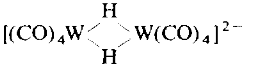 $[(CO)_4W\overset{H}{\underset{H}{<\,>}}W(CO)_4]^{2-}$	2.67
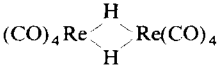 $(CO)_4Re\overset{H}{\underset{H}{<\,>}}Re(CO)_4$	1.52

2.75, 2.29 and 0.56 eV for the Mn, Mo and Cr complexes respectively (Table 5). This means that the bridge cores $Mo\overset{H}{\underset{H}{<\,>}}Mo$ and $Mn\overset{H}{\underset{H}{<\,>}}Mn$ are relatively stable and that the stability of the bridge core $Cr\overset{H}{\underset{H}{<\,>}}Cr$ is much lower. The $6b_{3u}$ level for $[(CO)_4Cr\overset{H}{\underset{H}{<\,>}}Cr(CO)_4]^{2-}$ lies so high that it mixes with the levels corresponding to the $d\mathrm{Cr} \rightarrow \pi^{a}\mathrm{CO}$ interactions (Fig. 2).

A typical feature of the manganese complex is that the $9a_g$ and $6b_{3u}$ orbitals are degenerate. This degeneration disappears when one of the bridging hydrogen atoms is replaced with the phosphine group. The bridge level $6b_{3u}$ is then replaced by lower levels corresponding to the bridge bond $Mn{-}PH_2{-}Mn$ (Fig. 3). This results in a higher stability of the $Mn\overset{PH_2}{\underset{H}{<\,>}}Mn$ core than the $Mn\overset{H}{\underset{H}{<\,>}}Mn$ core (Fig. 3). Similar stabilization of the bridge core in the carbonylmolybdenum dimer also occurs when one of the hydrogen atoms is replaced by phosphine or by any other bridging ligand. A comparison of the electronic structures of the $[(CO)_4Mo\overset{H}{\underset{H}{<\,>}}Mo(CO)_4]^{2-}$ and $[(CO)_4Mo\overset{H}{\underset{L}{<\,>}}Mo(CO)_4]^{2-}$ complexes, where L = OH, Cl, PH_2 will be covered extensively [11].

We now wish to compare the stabilization of bridge levels with regard to the HOMO level in the carbonyl dimers of chromium and molybdenum with double and single hydrogen bridges. In the $[(CO)_5M{-}H{-}M(CO)_5]^-$ complexes with D_{4h} symmetry, where M = Cr, Mo, only one filled molecular energy level $8a_{1g}$ corresponds to the M–H–M bridge bond [1]. As can be seen from Table 6 the

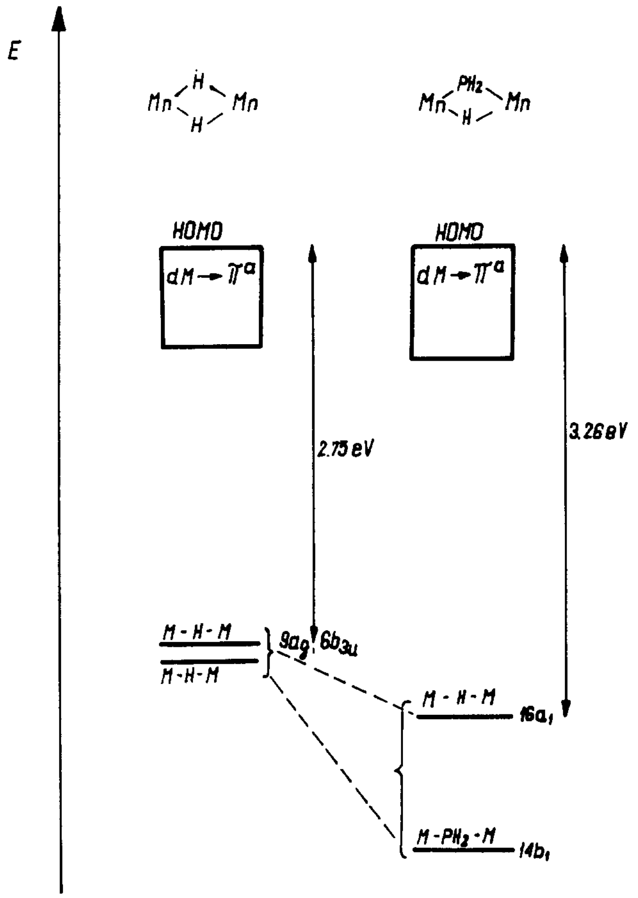

Fig. 3. Correlation of the molecular energy levels of $(CO)_4Mn\overset{H}{\underset{H}{\lessgtr}}Mn(CO)_4$ and $(CO)_4Mn\overset{PH_2}{\underset{H}{\lessgtr}}Mn(CO)_4$.

Table 6
Comparison of the stabilization of the bridge molecular energy levels in $[(CO)_5M{-}H{-}M(CO)_5]^-$ with D_{4h} symmetry and in $[(CO)_4M\overset{H}{\underset{H}{\lessgtr}}M(CO)_4]^{2-}$ with D_{2h} symmetry

Complex	Symmetry	$\Delta E_{HOMO,8a_{1g}}$ (eV)	$\Delta E_{HOMO,9a_{1g}}$ (eV)	$\Delta E_{HOMO,6b_{3u}}$ (eV)
$[(CO)_5Cr{-}H{-}Cr(CO)_5]^-$	D_{4h}	3.27	–	–
$[(CO)_4Cr\overset{H}{\underset{H}{\lessgtr}}Cr(CO)_5]^{2-}$	D_{2h}	–	2.36	0.56
$[(CO)_5Mo{-}H{-}Mo(CO)_5]^-$	D_{4h}	4.52	–	–
$[(CO)_4Mo\overset{H}{\underset{H}{\lessgtr}}Mo(CO)_4]^{2-}$	D_{2h}	–	3.88	2.29

stabilization of the $8a_{1g}$ bridge level with regard to the HOMO level in the complex

Table 7

Energies and compositions of highest occupied molecular energy levels of $(CH_3)_2Al\overset{H}{\underset{H}{<\;>}}Al(CH_3)_2$ with D_{2h} symmetry

MO	Energy (eV)	Greatest contributions by valence atomic orbitals (%)					
$2b_{2g}$ LUMO	6.84	p_x(Al)	93	p_x(C)	7		
$4a_g$ HOMO	−11.58	p_z(C)	46	p_y(C)	32	s(C)	13
$3b_{2u}$	−11.63	p_z(C)	45	p_y(C)	34	s(C)	14
$3b_{3g}$	−11.71	p_z(C)	48	p_y(C)	32	s(C)	14
$3b_{1u}$	−11.83	p_z(C)	45	p_y(C)	33	s(C)	14
$2b_{3g}$	−15.69	p_y(C)	34	p_z(C)	27	s(H)	24
$2b_{2u}$	−15.74	p_y(C)	33	p_z(C)	28	s(H)	23
$3a_g$	−16.30	p_y(C)	27	p_z(C)	24	s(H)	19
$2b_{1u}$	−16.89	p_y(C)	28	p_z(C)	23	s(H)	23
$2b_{3u}$	−18.65	$s(H_B)$	85	p_x(Al)	13	p_x(C)	2
$1b_{3u}$	−19.93	s(H)	52	p_x(C)	47		
$1b_{2g}$	−19.98	s(H)	51	p_y(C)	48		
$1b_{1g}$	−20.14	s(H)	52	p_x(C)	48		
$1a_u$	−20.18	s(H)	52	p_x(C)	48		
$2a_g$	−27.79	$s(H_B)$	59	s(Al)	32	p_z(Al)	8
$1a_g$	−27.90	s(H)	47	s(C)	44	s(Al)	5
$1b_{1u}$	−28.09	s(H)	49	s(C)	45	p_y(C)	2
$1b_{2u}$	−28.10	s(H)	55	s(C)	43	p_y(C)	2
$1b_{3g}$	−28.15	s(H)	53	s(C)	47		

with the single bridge for a particular metal is higher than that of the $9a_{1g}$ and $6b_{3u}$ levels in the complex with the double bridge.

Since the stability of the bridge core is determined by the stabilization of the bridge molecular levels it can be seen that in the carbonyl complexes of both chromium and molybdenum, the M–H–M bridge core is more stable than that of the $M\overset{H}{\underset{H}{<\;>}}M$ type.

We emphasize here that in the methyl hydride aluminium dimer $(CH_3)_2Al\overset{H}{\underset{H}{<\;>}}Al(CH_3)_2$ the electronic structure of the double hydrogen bridge is similar to that in the $[(CO)_4M\overset{H}{\underset{H}{<\;>}}M(CO)_4]^n$ complexes. The 1s AO of the bridging hydrogen atoms also participate in the formation of only two filled bonding bridge levels $2a_g$ and $2b_{3u}$ (Table 7). However, these levels differ from the analogous $9a_g$ and $6b_{3u}$ energy levels in carbonyl dimers in their localization on the bridge core with no terminal ligand contribution. In addition, the $2a_g$ and $2b_{3u}$ levels in $(CH_3)_2Al\overset{H}{\underset{H}{<\;>}}Al(CH_3)_2$ are separated by those of the terminal ligands while the analogous $9a_g$ and $6b_{3u}$ levels in $[(CO)_4M\overset{H}{\underset{H}{<\;>}}M(CO)_4]^n$ are not separated by any.

In $H_2B\overset{H}{\underset{H}{<\;>}}BH_2$ the 1s AO of the bridging hydrogen atoms participate in the

Table 8

Energies and compositions of highest occupied molecular energy levels of $H_2B\overset{H}{\underset{H}{<\,>}}BH_2$ with D_{2h} symmetry

MO	Energy (eV)	Greatest contributions by the valence atomic orbitals (%)					
$1b_{2g}$ LUMO	−1.76	p_x(B)	100				
$1b_{3g}$ HOMO	−18.66	s(H)	61	p_y(B)	39		
$1b_{2u}$	−19.52	p_y(B)	51	s(H)	49		
$2a_g$	−19.84	p_z(B)	44	s(H)	43	$s(H_B)$	9
$1b_{3u}$	−20.59	$s(H_B)$	51	p_x(B)	49		
$1b_{1u}$	−21.93	s(H)	51	s(B)	32	p_z(B)	17
$1a_g$	−26.07	s(B)	53	$s(H_B)$	31	p_z(B)	6

formation of three MOs: $1a_{1g}$, $1b_{3u}$ and $2a_g$ (Table 8). The bridge energy level $1a_{1g}$ is the lowest occupied energy level in the molecule.

The energy difference between the last filled level (HOMO) and the highest occupied bridge level is a measure of the hydrogen bridge stability in $(CH_3)_2Al\overset{H}{\underset{H}{<\,>}}Al(CH_3)_2$ and $H_2B\overset{H}{\underset{H}{<\,>}}BH_2$. So, it is characteristic that the stability of the double hydrogen bridge for the carbonyl dimers of transition metals and $H_2B\overset{H}{\underset{H}{<\,>}}BH_2$ is comparable. In $(CH_3)_2Al\overset{H}{\underset{H}{<\,>}}Al(CH_3)_2$ the double hydrogen bridge is much more stable and its stability is similar to the stability of the phosphine dimer of molybdenum [12].

The comparison of the stabilities of $H_2B\overset{H}{\underset{H}{<\,>}}BH_2$, $[(CO)_4Mo\overset{H}{\underset{H}{<\,>}}Mo(CO)_4]^{2-}$, $[(PH_3)_4Mo\overset{H}{\underset{H}{<\,>}}Mo(PH_3)_4]^{2+}$ and $(CH_3)_2Al\overset{H}{\underset{H}{<\,>}}Al(CH_3)_2$ is illustrated in Fig. 4. Each bonding molecular orbital in respect of the M–M axis corresponds to an antibonding orbital with respect to the M–M axis with the same contribution by the metal atomic orbitals (Tables 2, 3, 4, Fig. 5). Consequently the metal–metal overlap populations are close to zero (Table 9).

Because of this in complexes of the type $[(CO)_4M\overset{H}{\underset{H}{<\,>}}M(CO)_4]^n$, the group of last filled energy levels, which corresponds to the $d\mathrm{M} \rightarrow \pi^{a}\mathrm{CO}$ interaction, does not contribute to the direct metal–metal bond.

Thus, in carbonyl dimers with double hydrogen bridges the bonding between the metal atoms occurs only through the hydrogen bridge as in the single-hydrogen bridged transition metal carbonyls [1] as well as in $(CH_3)_2\overset{H}{\underset{H}{<\,>}}Al(CH_3)_2$.

Comparison of the results of the population analysis of $[(CO)_4M\overset{H}{\underset{H}{<\,>}}M(CO)_4]^n$ complexes (Table 9) shows that the overlap population of Mo–H is 0.147 and of Mn–H is 0.141, i.e. almost identical. We emphasize here that the overlap population

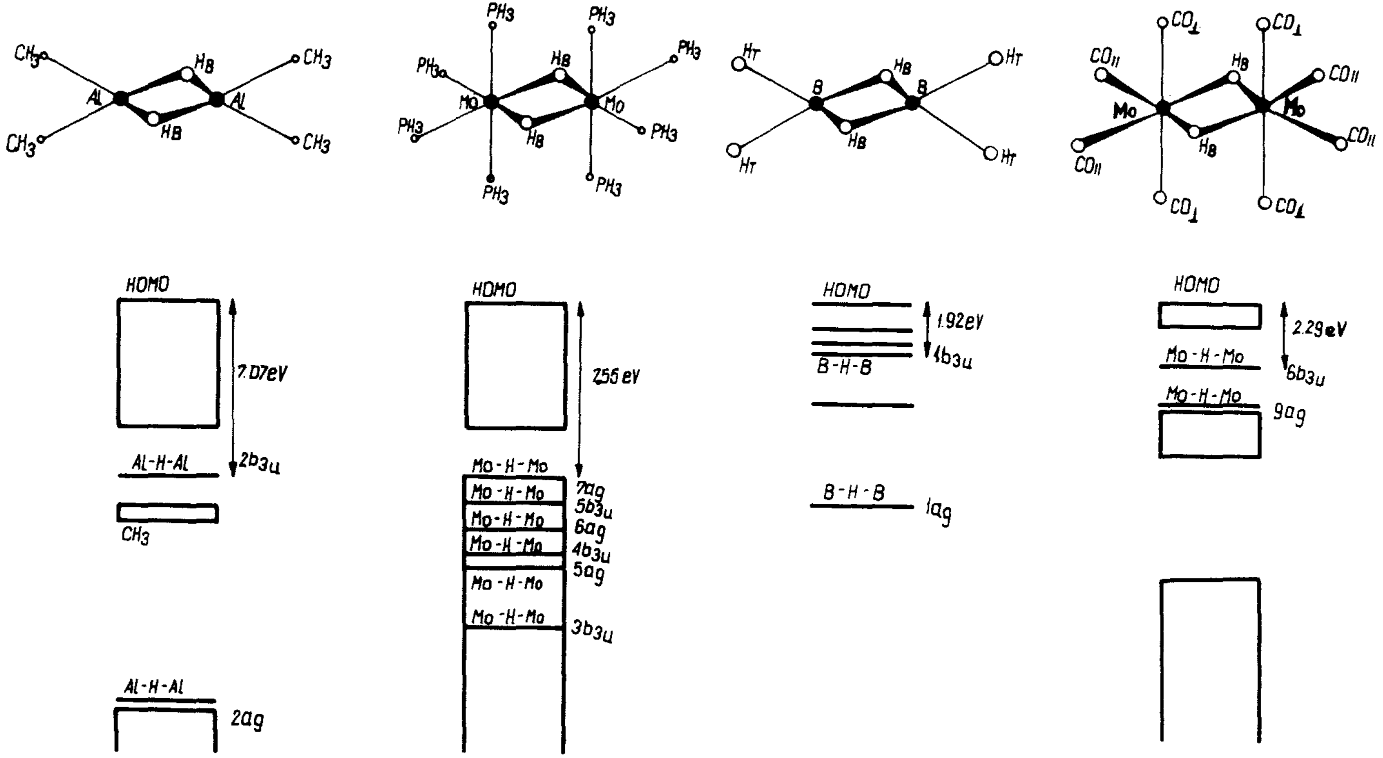

Fig. 4. Comparison of the stability of the double hydrogen bridge in $(\mathrm{CH_3})_2\mathrm{Al}\overset{\mathrm{H}}{\underset{\mathrm{H}}{\langle\rangle}}\mathrm{Al}(\mathrm{CH_3})_2$, $\mathrm{H_2B}\overset{\mathrm{H}}{\underset{\mathrm{H}}{\langle\rangle}}\mathrm{BH_2}$, $[(\mathrm{PH_3})_4\mathrm{Mo}\overset{\mathrm{H}}{\underset{\mathrm{H}}{\langle\rangle}}\mathrm{Mo}(\mathrm{PH_3})_4]^{2+}$ and $[(\mathrm{CO})_4\mathrm{Mo}\overset{\mathrm{H}}{\underset{\mathrm{H}}{\langle\rangle}}\mathrm{Mo}(\mathrm{CO})_4]^{2-}$.

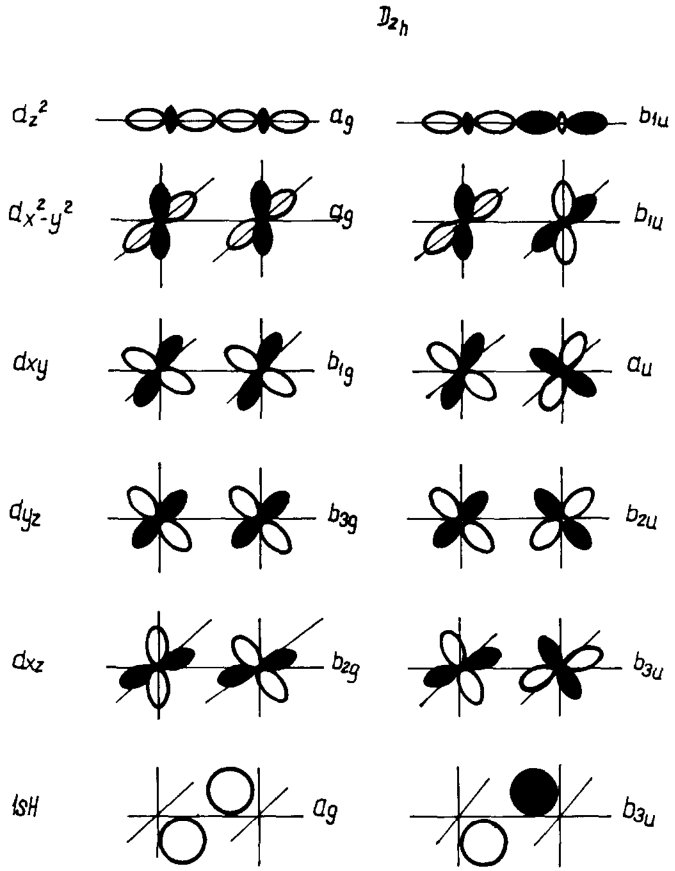

Fig. 5. Symmetry-adapted linear combinations of the *d* atomic orbitals of the metal and hydrogen atoms.

of Al–H in $(CH_3)_2Al\overset{H}{\underset{H}{\langle\,\rangle}}Al(CH_3)_2$ determined by the Fenske-Hall method is 0.149 (Table 9). This is indicative of the same covalent character of the Mo–H–Mo, Mn–H–Mn and Al–H–Al bonds in the compounds discussed above. On the other hand, the much lower overlap population of Cr–H of 0.65 results from a lower contribution by the *s* and *p* atomic orbitals of Cr in the bridge bond than that for Mo and Mn since the overlap populations of *d* type metal orbitals with the 1*s* orbitals of the bridging hydrogen atoms, i.e. *d*M–1*s*H are all of the same order for Cr,Mo and Mn (Table 9).

The distribution of the atomic charges is similar for the $Cr\overset{H}{\underset{H}{\langle\,\rangle}}Cr$ and $Mo\overset{H}{\underset{H}{\langle\,\rangle}}Mo$ bridge cores. The metal atoms have fairly high positive charges, and the hydrogen atoms bear fairly high negative charges (Table 10).

This indicates partial ionic character of the Cr–H–Cr and Mo–H–Mo bonds in the complexes under examination and in this respect they most resemble the

Table 9
Mulliken overlap populations

Compound	Overlap populations							
	M–M	M–H_B	dM–H_B	M–$C_\parallel$	M–$C_\perp$	dM–$C_\parallel$	dM–$C_\perp$	H_B–H_B
Calculated by use of the Fenske-Hall method								
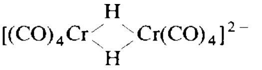 $[(CO)_4Cr\overset{H}{\underset{H}{\lt\gt}}Cr(CO)_4]^{2-}$	0.000	0.066	0.061	0.287	0.296	0.233	0.200	−0.004
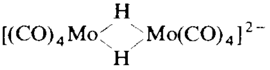 $[(CO)_4Mo\overset{H}{\underset{H}{\lt\gt}}Mo(CO)_4]^{2-}$	0.023	0.147	0.061	0.395	0.418	0.247	0.222	−0.017
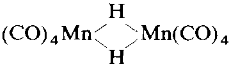 $(CO)_4Mn\overset{H}{\underset{H}{\lt\gt}}Mn(CO)_4$	0.032	0.141	0.051	0.421	0.397	0.237	0.190	−0.002
	Al–Al	Al–H_B	Al–C					
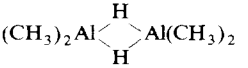 $(CH_3)_2Al\overset{H}{\underset{H}{\lt\gt}}Al(CH_3)_2$	0.074	0.150	0.162	–	–	–	–	−0.044
	B–B	B–H_B	B–H					
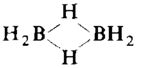 $H_2B\overset{H}{\underset{H}{\lt\gt}}BH_2$	0.186	0.217	0.436					
Calculated by use of the EHT method								
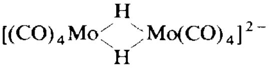 $[(CO)_4Mo\overset{H}{\underset{H}{\lt\gt}}Mo(CO)_4]^{2-}$	0.066	0.301	–	0.839	0.837			
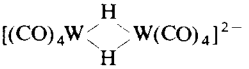 $[(CO)_4W\overset{H}{\underset{H}{\lt\gt}}W(CO)_4]^{2-}$	0.108	0.319	–	0.933	0.814			
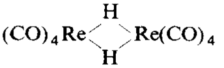 $(CO)_4Re\overset{H}{\underset{H}{\lt\gt}}Re(CO)_4$	0.143	0.320	–	0.787	0.789			

Al–H–Al bond in 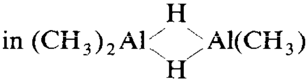 $(CH_3)_2Al\overset{H}{\underset{H}{\lt\gt}}Al(CH_3)_2$ (Table 10). Yet the Mn–H–Mn bond is exclusively covalent like the B–H–B in 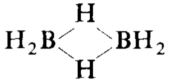 $H_2B\overset{H}{\underset{H}{\lt\gt}}BH_2$ since the negative charges are localized on both the hydrogen and manganese atoms and the positive charges are localized on both the boron and hydrogen atoms (Table 10).

It is also interesting to compare the electronic density distribution for the bridge cores in the 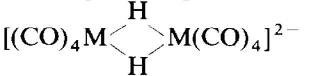 $[(CO)_4M\overset{H}{\underset{H}{\lt\gt}}M(CO)_4]^{2-}$ and $[(CO)_5M{-}H{-}M(CO)_5]^-$ complexes, where M = Cr, Mo. This comparison is presented in Table 11. Thus, an increase in the hydrogen bridge multiplicity for the same type of complexes does not actually result in a change in the negative charges on the bridging hydrogen atoms. However, the positive charges on the metal atoms increase considerably and consequently the ionic character of the M–H–M bond increases too. On the contrary, its covalent character remains unchanged.

Table 10
Mulliken atomic charges

Compound	Atomic charges			
	M	H_B	$CO_{\parallel}$	$CO_{\perp}$
Calculated by use of the Fenske-Hall method				
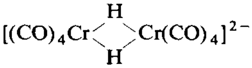 $[(CO)_4Cr\overset{H}{\underset{H}{<>}}Cr(CO)_4]^{2-}$	0.954	−0.435	−0.412	−0.358
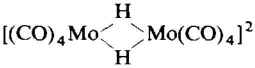 $[(CO)_4Mo\overset{H}{\underset{H}{<>}}Mo(CO)_4]^{2-}$	0.746	−0.331	−0.391	−0.316
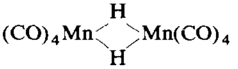 $(CO)_4Mn\overset{H}{\underset{H}{<>}}Mn(CO)_4$	−0.060	−0.178	−0.058	0.177
	Al	H_B	CH_3	
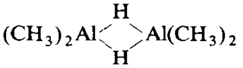 $(CH_3)_2Al\overset{H}{\underset{H}{<>}}Al(CH_3)_2$	1.837	−0.506	0.135	
	B	H_B	H	
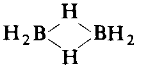 $H_2B\overset{H}{\underset{H}{<>}}BH_2$	0.046	0.083	−0.065	
Calculated by use of the EHT method				
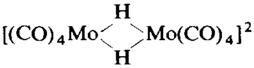 $[(CO)_4Mo\overset{H}{\underset{H}{<>}}Mo(CO)_4]^{2-}$	1.319	−0.330	−0.604	−0.609
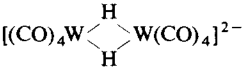 $[(CO)_4W\overset{H}{\underset{H}{<>}}W(CO)_4]^{2-}$	0.384	−0.358	−0.436	−0.078
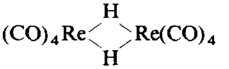 $(CO)_4Re\overset{H}{\underset{H}{<>}}Re(CO)_4$	−0.870	−0.219	0.268	0.277

The analysis of the electron density distribution on the terminal ligands indicates that for the complexes 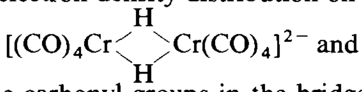 $[(CO)_4Cr\overset{H}{\underset{H}{<>}}Cr(CO)_4]^{2-}$ and 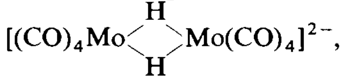 $[(CO)_4Mo\overset{H}{\underset{H}{<>}}Mo(CO)_4]^{2-}$, negative charges on the carbonyl groups in the bridge plane ($CO_{\parallel}$) are larger than those on the carbonyl groups situated in the plane perpendicular to the hydrogen bridge ($CO_{\perp}$) (Table 10). This indicates that the $dM \rightarrow \pi^{a}CO_{\parallel}$ type interactions are stronger than those of the $dM \rightarrow \pi^{a}CO_{\perp}$ type. This should lead to elongation of the $M{-}CO_{\perp}$ bond with respect to $M{-}CO_{\parallel}$ which is indicative of the *cis* effect of the bridging hydrogen atoms. In fact, for the analogous tungsten complex, 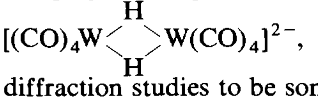 $[(CO)_4W\overset{H}{\underset{H}{<>}}W(CO)_4]^{2-}$, the $M{-}CO_{\perp}$ bonds (1.995 Å) were found by X-ray diffraction studies to be somewhat longer than the $M{-}CO_{\parallel}$ bonds (1.950 Å) [4]. On the other hand, for the manganese complex negative charges on the $CO_{\parallel}$ groups are smaller than those in the Cr and Mo complexes whereas charges on the $CO_{\perp}$ groups are actually positive. This results from a higher contribution by $\sigma CO{-}Mn$ interactions to the $Mn{-}CO_{\perp}$ bond than by the $dMn \rightarrow \pi^{a}$ interactions.

In fact, the percentage contribution by the *ns*, *np* atomic orbitals of manganese in the formation of molecular levels which correspond to σCO interactions is higher than in the case of chromium and molybdenum (Tables 2, 3, 4).

Table 11

Comparison of the electronic density distribution for the bridge cores in the 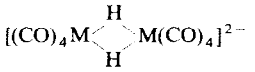 $[(CO)_4M\overset{H}{\underset{H}{\diamond}}M(CO)_4]^{2-}$ and $[(CO)_5M{-}H{-}M(CO)_5]^-$ complexes

Compound:	$[(CO)_5Cr{-}H{-}Cr(CO)_5]^-$	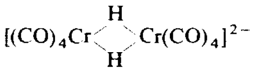 $[(CO)_4Cr\overset{H}{\underset{H}{\diamond}}Cr(CO)_4]^{2-}$	$[(CO)_5Mo{-}H{-}Mo(CO)_5]^-$	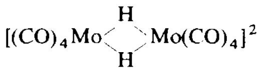 $[(CO)_4Mo\overset{H}{\underset{H}{\diamond}}Mo(CO)_4]^{2-}$
Symmetry:	D_{4h}	D_{2h}	D_{4h}	D_{2h}
Atomic charges				
M	0.596	0.954	0.344	0.746
H_B	−0.499	−0.435	−0.346	−0.331
Overlap populations				
M–M	−0.002	0.000	0.006	0.023
$M{-}H_B$	0.070	0.066	0.149	0.147

Electronic structure of the $[(CO)_4M\underset{H}{\overset{H}{<\;>}}M(CO)_4]^n$ *complexes determined by use of the EHT method*

In general the energy level diagrams for the carbonyl dimers with double hydrogen bridges of the $[(CO)_4M\underset{H}{\overset{H}{<\;>}}M(CO)_4]^n$ type, where M = Mo, W, $n = 2$ or M = Re, $n = 0$ determined by the EHT method resemble the energy level diagrams determined for those complexes by the Fenske-Hall method. There are some differences in the group of molecular levels corresponding to the bridge bonds.

Figure 2 depicts the energy levels determined by use of the Fenske-Hall and the EHT methods for $[(CO)_4Mo\underset{H}{\overset{H}{<\;>}}Mo(CO)_4]^{2-}$ and the energy levels determined by use of the EHT method for $[(CO)_4W\underset{H}{\overset{H}{<\;>}}W(CO)_4]^{2-}$ and $(CO)_4Re\underset{H}{\overset{H}{<\;>}}Re(CO)_4$. For the molybdenum complex, the HOMO energy levels calculated by use of each method are almost equal.

The energy levels $5a_g$ and $6b_{3u}$, which correspond to the bridge bonds in $[(CO)_4Mo\underset{H}{\overset{H}{<\;>}}Mo(CO)_4]^{2-}$, determined by use of the EHT method have almost the same percentage composition and almost the same energy range as the similar $9a_g$ and $6b_{3u}$ levels determined by use of the Fenske-Hall method. However the $5a_g$ and $6b_{3u}$ levels are separated by the group of non-bonding energy levels that correspond to the σ and π^b MOs of the terminal CO groups. One can assume that their separation results from specific properties of the EHT method used, whereby the energy of terminal ligands is usually overestimated.

For the complexes of rhenium and tungsten the atomic orbitals of the bridging hydrogen atoms provide a significant contribution to the formation of more than two filled bridge levels which differ only slightly in their energies. These are the $5a_g$, $7a_g$, $5b_{3u}$, $8a_g$ and $6b_{3u}$ levels for $[(CO)_4W\underset{H}{\overset{H}{<\;>}}W(CO)_4]^{2-}$ and the $5a_g$, $3b_{3u}$, $7a_g$, $5b_{3u}$, $9a_g$ and $6b_{3u}$ levels for $(CO)_4Re\underset{H}{\overset{H}{<\;>}}Re(CO)_4$.

The contribution by the $1s$ orbitals of the bridging hydrogen atoms to each of these levels is 30 to 50% for the tungsten complex, and 20 to 30% for the rhenium complex.

The energy levels which correspond to the bridge bonds are intermixed with those of the σ and π type from the CO groups. We believe, that this delocalization of $1s$H orbitals results from overestimation of the energy levels of the terminal ligands orbitals. This is also supported by the fact that all bridge levels for $[(CO)_4W\underset{H}{\overset{H}{<\;>}}W(CO)_4]^{2-}$ and $(CO)_4Re\underset{H}{\overset{H}{<\;>}}Re(CO)_4$ are in the same energy range as the corresponding $5a_g$ and $6b_{3u}$ levels for $[(CO)_4Mo\underset{H}{\overset{H}{<\;>}}Mo(CO)_4]^{2-}$ (Fig. 2).

The stabilization energies of the $6b_{3u}$ bridge level with respect to the HOMO level are 2.67, 1.66 and 1.52 eV for tungsten, molybdenum and rhenium complexes, respectively (Table 5). This results in the comparable stability of the bridge cores $\mathrm{Mo}\overset{\mathrm{H}}{\underset{\mathrm{H}}{\langle\;\rangle}}\mathrm{Mo}$ and $\mathrm{Re}\overset{\mathrm{H}}{\underset{\mathrm{H}}{\langle\;\rangle}}\mathrm{Re}$ and in the greater stability of the $\mathrm{W}\overset{\mathrm{H}}{\underset{\mathrm{H}}{\langle\;\rangle}}\mathrm{W}$ core.

When the above-mentioned results of calculations by the Fenske-Hall method are taken into account, it becomes evident that the stability of the $\mathrm{M}\overset{\mathrm{H}}{\underset{\mathrm{H}}{\langle\;\rangle}}$ bridge core depends on the type of metal, in the order:

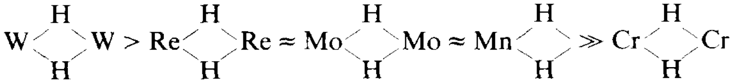

$$\mathrm{W}\overset{\mathrm{H}}{\underset{\mathrm{H}}{\langle\;\rangle}}\mathrm{W} > \mathrm{Re}\overset{\mathrm{H}}{\underset{\mathrm{H}}{\langle\;\rangle}}\mathrm{Re} \approx \mathrm{Mo}\overset{\mathrm{H}}{\underset{\mathrm{H}}{\langle\;\rangle}}\mathrm{Mo} \approx \mathrm{Mn}\overset{\mathrm{H}}{\underset{\mathrm{H}}{\langle\;\rangle}} \gg \mathrm{Cr}\overset{\mathrm{H}}{\underset{\mathrm{H}}{\langle\;\rangle}}\mathrm{Cr}$$

The results of a population analysis suggest the same conclusions as in the case of calculations by the Fenske-Hall method (Tables 10, 11). Thus, the overlap population of M–H does not depend on the type of metal, which indicates that the same covalency is present in Mo–H–Mo, W–H–W and Re–H–Re bonds. In addition, the Mo–H–Mo and W–H–W bonds are partly ionic since the hydrogen atoms have negative charge and the molybdenum and tungsten atoms have positive charges. By contrast the Re–H–Re bond has an exclusively covalent nature analogous to that of the Mn–H–Mn bond since there is negative charge on both the rhenium and hydrogen atoms. The overlap population values of M–M for the complexes of Mo, W and Re are low and this indicates a very weak direct bond between the metal atoms.

Positive charges on the terminal ligands $\mathrm{CO}_{\perp}$ and $\mathrm{CO}_{\parallel}$, in $(\mathrm{CO})_4\mathrm{Re}\overset{\mathrm{H}}{\underset{\mathrm{H}}{\langle\;\rangle}}\mathrm{Re(CO)}_4$ indicate a higher contribution of the σCO–M interaction in the Re–$\mathrm{CO}_{\perp}$ and Re–$\mathrm{CO}_{\parallel}$ bonds compared with those of the $d\mathrm{M} \rightarrow \pi^{a}\mathrm{CO}$ type, like that in the manganese complex.

Conclusions

Thus we have found that there is practically no direct M–M bond in the chromium, molybdenum, manganium, rhenium and tungsten carbonyl dimers with double hydrogen bridges. The metal atoms are bonded exclusively through the hydrogen bridge, like that in the carbonyl dimers with single hydrogen bridge.

The double hydrogen bridge stability for the Mo, W, Mn and Re complexes is similar and comparable with the stability of the double hydrogen bridge in the $\mathrm{H_2B}\overset{\mathrm{H}}{\underset{\mathrm{H}}{\langle\;\rangle}}\mathrm{BH_2}$, but in the chromium complex it is considerable less stable.

The covalent character of the M–H–M bridge bond is the same for all complexes discussed here, however ionic character depends on the type of metal since the charge on the hydrogen atom is always negative in these complexes.

An increase in the hydrogen multiplicity for the same type of complexes causes an increase in the ionic character of the M–H–M bond, while maintaining its covalent character, and a decrease in hydrogen bridge stability.

In these complexes we found the *cis* effect of the bridging hydrogen atom similar as in the carbonyls with single hydrogen bridge.

Acknowledgement

This work was supported financially by Project No. CPBP 01.12 of Polish Academy of Sciences.

References

1 B. Jeżowska-Trzebiatowska and B. Nissen-Sobocińska, J. Organomet. Chem., 322 (1987) 331.
2 M.B. Hall and R.F. Fenske, Inorg. Chem., 11 (1972) 768.
3 (a) R. Bau, R.G. Teller and S.W. Kirtley, Acc. Chem. Res., 12 (1976) 176; (b) R. Bau and T.F. Koetzle, Pure Appl. Chem., 50 (1978) 55; (c) R.A. Love, H.B. Chin, T.F. Koetzle, S.W. Kirtley, B.R. Whittlesey and R. Bau, J. Am. Chem. Soc., 98 (1976) 4493; (d) J. Rozière, J.M. Williams, R.P. Stewart, J.L. Petersen and L.F. Dahl, J. Am. Chem. Soc., 99 (1977) 4497; (e) J.L. Petersen, P.L. Johnson, J. O'Connor, L.F. Dahl and J.M. Williams, Inorg. Chem., 17 (1978) 3460.
4 M.R. Churchill and S.W.Y. Chang, Inorg. Chem., 13 (1974) 2413.
5 M.J. Bennett, W.A.G. Graham, J.K. Hoyano and W.L. Hutcheon, J. Am. Chem. Soc., 94 (1972) 6232.
6 J.L. Petersen and J.M. Williams, Inorg. Chem., 17 (1978) 1308.
7 R.J. Doedens, W.T. Robinson and J.A. Ibers, J. Am. Chem. Soc., 89 (1967) 4323.
8 A. Dedieu, T.A. Albright and R. Hoffmann, J. Am. Chem. Soc., 101 (1979) 3141.
9 L.S. Bartell and B.L. Carrol, J. Chem. Phys., 42 (1965) 1135.
10 A. Almeningen, G.A. Anderson, G.A. Forgaard and F.R. Halland, Acta Chem. Scand., 26 (1972) 2315.
11 B. Jeżowska-Trzebiatowska and B. Nissen-Sobocińska, submitted.
12 B. Jeżowska-Trzebiatowska and B. Nissen-Sobocińska, submitted.